Carrier Transport Induced and Controlled by Defects

Contents

Abstract

With a large density of impurities or other lattice defects, the carrier transport deviates substantially from the classical transport within the band. It is carried within energy ranges (within the bandgap), which are determined by the defect structure. *Heavy doping* produces predominant defect levels split into two impurity bands. Below a density to permit sufficient tunneling, carrier transport requires excitation into the conduction band; at higher defect density, a diffusive transport within the upper impurity band becomes possible. At further increased defect density, metallic conductivity within the then unsplit impurity band occurs.

In *amorphous semiconductors*, tunneling-induced carrier transport can take place within the tail of states, which extend from the conduction or valence band into the bandgap. Major carrier transport starts at an energy referred to as the

K.W. Böer, U.W. Pohl, *Semiconductor Physics*,
https://doi.org/10.1007/978-3-319-69150-3_28

mobility edge. With statistically distributed defects, only some volume elements may become conductive. These volume elements widen at increasing temperature, eventually providing an uninterrupted *percolation path* through a highly doped or disordered semiconductor with a density-related threshold of conduction.

Conductance in *organic semiconductors* is governed by static and dynamic disorder. Band conductance in small-molecule crystals shows a decreasing carrier mobility at increased temperature with a power law similar to that of inorganic semiconductors. Small-molecule or polymer semiconductors with dominating static disorder show hopping conductance with a typically low but increasing mobility at higher temperatures.

Keywords

Amorphous semiconductor · Band conductance · Dispersive transport · Heavy doping · Hopping conduction · Hopping mobility · Impurity band · Mobility edge · Organic semiconductor · Percolation · Phonon-activated conduction · Tunneling-induced transport · Variable-range hopping

1 Impurity-Band Conduction

In addition to causing scattering, lattice defects can contribute directly to the carrier transport in two ways. They permit direct quantum-mechanical exchange of carriers from defect to defect (i.e., tunneling from one trap level to the next), or by thermal ionization of a carrier from a trap level into the band, intermediate transport within the band, and then a retrapping as shown in Fig. 1. The first type of carrier transport is called *tunneling* or *impurity-band conduction*; the second type is known as *hopping conduction* or *phonon-activated conduction.* These types of carrier transport are of major importance in highly disordered, highly doped, or amorphous semiconductors. For reviews, see Shklovskii and Efros (1984) and Mott (1993).

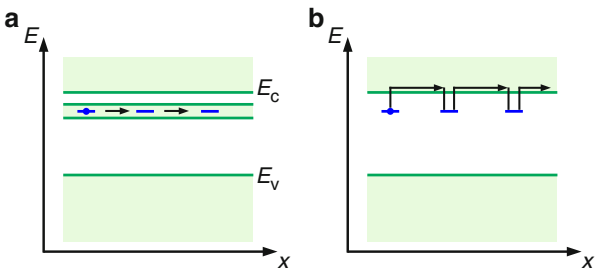

Fig. 1 (**a**) Impurity-band conduction and (**b**) hopping conduction in highly doped semiconductors

1.1 Concept of Impurity Bands

In a rather simple model, the overlapping hydrogen-like donor states can be used to form a *Hubbard band* (Hubbard 1963), which is centered about their ground-state energy. With partial compensation, there are $N_d - N_a$ free states in this Hubbard band, and conduction can occur (Adler 1980). The band width ΔE_B is given by the overlap integral between equal centers at distance $1/\sqrt[3]{N}$, where N is the density of uncompensated donors ($= N_d - N_a$). This bandwidth is roughly equal to the interaction energy

$$\Delta E_B \cong \frac{e^2 \sqrt[3]{N}}{4\pi\varepsilon_{stat}\varepsilon_0}. \tag{1}$$

The effective mass within this narrow impurity band is much larger than in the adjacent carrier band; hence, the *impurity-band mobility* is usually quite small ($< 10^{-2}$ cm^2/(Vs)). The mobility-effective mass in this impurity band should not be confused with the effective mass of a Bloch electron within the conduction band, which is hence related to each quasihydrogen state of the donor.

The carrier transport within such a narrow impurity band can no longer be described by the Boltzmann equation. The carrier transport must now be evaluated from the quantum-mechanical expectation value for the current, which is given by the *Kubo formula* (Kubo 1956, 1957). A somewhat simplified version was developed by Greenwood (1958) in which the conductivity can be expressed as

$$\sigma = -\int \sigma_0(E) \frac{\partial f}{\partial E} dE, \tag{2}$$

with

$$\sigma_0(E) = \frac{2\pi e^2 \hbar^2 V}{m_n^2} \{g(E)\}^2 \left| \int \psi * (E') \frac{\partial}{\partial \mathbf{r}} \psi(E) d\mathbf{r} \right|^2, \tag{3}$$

being proportional to $g(E)$, the density of states, and the matrix element describing the electron transitions from E to E'; f is the Fermi distribution function and V is the sample volume. Equation 2 is referred to as the *Kubo-Greenwood formula*, which, when evaluated for $E = E'$, gives the tunneling current between equivalent defect centers.

The distance between the impurities is not constant but fluctuates statistically; the impurity band is therefor substantially undulated. It is broader where impurities are closer together and narrower where they are more widely spaced.

Since there is no scattering during the tunneling process between adjacent defects, the tunneling is essentially temperature-independent. Except for thermal expansion, which has a small influence on the average distance between defects, and except for the broadening of the defect levels with increased lattice oscillation, the *trap conductivity* is almost temperature-independent when the Fermi level lies close to the extended states. Trap conductivity is important in highly doped semiconductors,

semiconducting glasses, and inorganic semiconductors, that is, in all semiconductors with a high density of defects (see Sect. 4).

When carriers are created by optical excitation, trap conductivity persists to low temperatures and has a quasi-metallic behavior (Mott and Davis 1979). We will now describe in more detail the impurity band.

1.2 The Impurity Band

In semiconductors with high doping densities ($> 10^{18}$ cm^{-3}), shallow donors or acceptors can come close enough (<100 Å) to each other so that their eigenfunctions overlap significantly and therefore permit the exchange of carriers directly, without the involvement of the adjacent bands. Consequently, the defect level is split and develops into a narrow *impurity band*-see Fig. 1a. Such impurity-band formation is a basic effect that occurs whenever a defect level is present at sufficient density. The formation of an impurity band is widely applied in blocked-impurity-band devices, where a heavily – but not degenerately – donor-doped layer creates an impurity band; this region is used as an infrared-active layer in IR photo detectors, where an incoming photon lifts an electron from the impurity band to the conduction band (Haegel et al. 2003, Wang et al. 2015).

The term "band" should, however, be used with caution, as it requires a more detailed density-of-states analysis and a distinction between localized and delocalized states; the latter are true band states. In principle, the Anderson Model (▶ Sect. 1.1 of chapter "Defects in Amorphous and Organic Semiconductors") should be used to obtain some information about the localization aspect of the states. We will first discuss this behavior in a rather general fashion.

1.2.1 The Lifshitz-Ching-Huber Model

In the Lifshitz model, a statistical distribution of N identical potential wells is analyzed to obtain a density-of-states distribution of these defect levels and to identify a critical density at which the states within the center of the distribution become delocalized (Lifshitz 1965). This model is a forerunner of the Mott version, which is used to distinguish localized and nonlocalized states in band tails, see ▶ Sect. 1.2 of chapter "Defects in Amorphous and Organic Semiconductors" and Sect. 4.1.

When two identical defect centers are brought together, they show a split of eigenstates of the form

$$\psi_s = \frac{1}{\sqrt{2}}(\phi_1 + \phi_2) \quad \text{and} \quad \psi_a = \frac{1}{\sqrt{2}}(\phi_1 - \phi_2) \quad \text{with} \quad E_s - E_a = 2I, \tag{4}$$

where ϕ_1 and ϕ_2 are the wavefunctions of the two centers, E_s and E_a are the energies of the symmetric and antisymmetric states ψ_s and ψ_a, respectively, and I is the transfer integral (▶ Eq. 2 of chapter "Defects in Amorphous and Organic Semiconductors"). When a third center is approaching at an arbitrary distance, it will not,

however, participate in the resonance splitting. This is due to the fact that the doublet of the two centers closest to each other is far enough apart to be out of resonance with the third center. Hence, the Lifshitz model yields a band of *localized* states for statistically distributed traps. Only when these defects are close enough to fulfill

$$N^{1/3} r_0 \cong 0.3, \tag{5}$$

with r_0 as the fall-off radius of the wavefunction of an isolated defect ($= a_{\mathrm{qH}}$ for a hydrogen-like defect) can delocalization of the states in the center of the band occur (Ching and Huber 1982). This result is close to the Mott-Anderson result for localization (see ▶ Eq. 17 of chapter "Defects in Amorphous and Organic Semiconductors". When interacting with each other, the splitting of the defect states also gives rise to a splitting of this defect band, causing the density of states to have a minimum near the center of the distribution.

1.2.2 Coulomb Gap and Mott Transition

The density minimum of the defect levels near the center of the density-of-states distribution may become complete in (partially) compensated semiconductors with a gap between filled and empty states. Such splitting is caused by the long-range Coulomb interaction of *localized* electrons (Knotek and Pollak 1974; Efros and Shklovskii 1975) and occurs at the position of the Fermi level. For an inclusion of static screening, see Mazuruk et al. (1989); such screening affects the density of states at the Fermi level and can replace the Coulomb gap by a dip in the density of states.

It can be shown that the Coulomb gap appears only for *localized* states. When the density of states becomes large enough, so that delocalization occurs (see below), then the Coulomb gap disappears (Aronov et al. 1979; Altshuler et al. 1980).

The impurity band with localized states cannot contribute to the conductivity at $T = 0$ K since it has an energy gap between filled and empty states. When the density of impurities is increased to an extent that delocalization occurs at the Fermi level, the gap disappears, and quasi-metallic conductivity is observed. This transition within an impurity band is a *Mott-transition* and is related to a critical conductivity that was termed by Mott as *minimum metallic conductivity*

$$\sigma_{\min} \cong 0.05 \frac{e^2}{\hbar} N_{\mathrm{Mott}}^{1/3}, \tag{6}$$

where N_{Mott} is the critical doping density–see below (Mott and Davis 1979). The Mott transition is observed to be smooth rather than abrupt, probably because of density fluctuation of impurities.

For Si:P, the Mott-transition occurs at a critical donor density of $N_{\mathrm{Mott}} = 3.7 \times 10^{18}$ cm^{-3}; for this example, we obtain $\sigma_{\min} \cong 20\ \Omega^{-1}$ cm^{-1} (Rosenbaum et al. 1980) (see also ▶ Sect. 3.2 of chapter "Equilibrium Statistics of Carriers").

Scaling When, for example, hydrogen-like donors are close enough to each other, the donors' electrons no longer belong to a certain donor, but are able to move freely between donors even at $T = 0$ K, like electrons in a metal; that is, they belong to all of the donors. Critical to this transition are three units of length: the inter-donor distance $1/\sqrt[3]{N}$, the quasi-hydrogen radius a_{qH}, and the mean free path λ – for a diffusion-type of carrier migration. Their relative magnitude determines the type of conductivity, and its discussion is a subject of the theory of scaling. For a recent tight-binding analysis of localization in 3D to 1D systems with hopping matrix-elements that decay exponentially in the separation distance between neighboring sites, see Priour (2012); extended states in 3D are found to occur even for small decay lengths, but the interval of energies supporting extended states decreases exponentially for decreasing decay length.

Abrahams et al. (1979) suggested to use a dimensionless conductance of a cube of length L rather than the conductivity

$$G = \sigma L \times \frac{2\hbar}{e^2}, \tag{7}$$

measured in elementary units of $2\hbar/e^2$. They discussed the changes in G as a function of L; it should change when L approaches atomic dimensions. They argued that the scaling function

$$\beta(G) = \frac{\partial \ln G}{\partial \ln L} \tag{8}$$

is a universal function (Thouless 1974, 1980), which is ~1 for large conductances, becomes zero at a critical conductance G_{c}, and turns negative for $G < G_{\mathrm{c}}$–see Fig. 2. Within this theory, G_{c} is a universal constant[1] and indicates the transition between metal-like and semiconductor-type conductivity. Here, Mott obtains for the critical conductivity

$$\sigma_{\mathrm{c}} \cong 0.03 \frac{e^2}{\hbar\ a_{\mathrm{qH}}}, \tag{9}$$

a value close to $\sigma_{\min}$ given by Eq. 6, here for $\sqrt[3]{N_{\mathrm{Mott}}} \cong 1/a_{\mathrm{qH}}$.

Ioffe-Regel Rule For a further discussion of the concept of minimum metallic conductivity, we start from a metal and look for candidates of lower and lower mean free paths, that is, reduced conductivities. There are indications that with increased lattice disturbance, lower conducting metals (such as liquid metals) have a lower mean free path, but with a lower limit equal to the interatomic

[1]It should, however, depend on the microscopic atomic arrangement and on the coordination (Mott and Kaveh 1985).

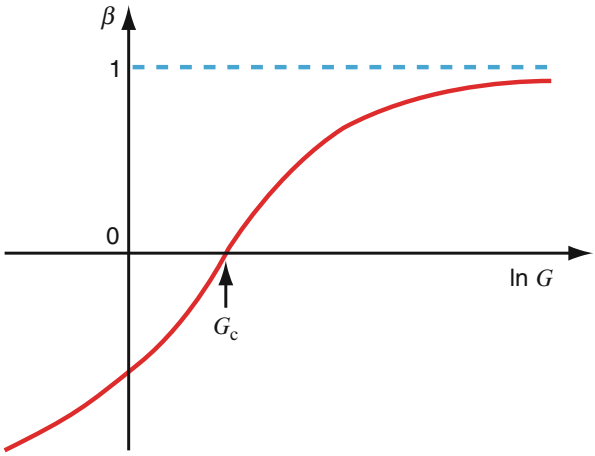

Fig. 2 Scaling function versus the dimensionless conductance (Eq. 7) for a 3D semiconductor

distance. The *Ioffe-Regel rule* argues that the electron wavefunction cannot lose phase memory faster than on the order of the interatomic distance a (Ioffe and Regel 1960). This means that the conductivity of a metal cannot be smaller than $\sigma = e\,\mu\,n$, with $n = a^{-1/3}$ and $\mu = (e/m_n)\,\tau = (e/m_n)\,(a/v_F)$. The Fermi-momentum is given by $\hbar\,k_F = m_n\,v_F = m_n(3\pi^2 n)^{1/3}$; hence, one obtains as minimum metallic (Ioffe-Regel) conductivity

$$\sigma_{\text{I-R}} = \frac{1}{\sqrt[3]{3\pi^2}}\,\frac{e^2}{\hbar\,a} = 0.32\,\frac{e^2}{\hbar\,a}\,. \tag{10}$$

In doped semiconductors, two changes need to be introduced:

1. Instead of the interatomic distance, the quasi-hydrogen radius applies
2. Only a certain fraction of the impurity-band states are extended states, which, after Mott and Kaveh (1985), is on the order of 8.5%, yielding Eq. 9 as critical conductivity in a semiconductor. For $a_{qH} \cong 30$ Å, this critical conductivity is on the order of 20 Ω^{-1} cm^{-1}.

Carrier Localization in Strong Electric Fields When carriers are transported in narrow bands, independent of how such bands are produced, carrier localization can occur when the electric field is strong enough. Here, stationary electron states become localized in the direction of the electric field due to reflection at the boundaries of the Brillouin zone (Wannier 1960). This causes a *Stark ladder*, with the possibility of phonon-induced jumps between the levels of this ladder (Hacker and Obermair 1970). Resonance effects occur when the steps become equal to LO phonons (Maekawa 1970), causing current oscillations.

Another possibility of carrier localization occurs for small polarons in strong electric fields, where the mobility decreases with increasing field in the tunneling

regime (Böttger and Bryksin 1979, 1980). For electric-field-induced carrier localization in one-dimensional semiconductors, see Pronin et al. (1994).

2 Phonon-Activated Conduction

For sufficiently high densities of impurities, the carrier transport within an impurity band occurs with a mean free path longer than the spacing of impurities. With less doping, the defect levels will become localized, and conduction can occur in one of two fashions:

1. By tunneling from one defect to the nearest neighboring defect of the same type
2. After thermal excitation into the adjacent band

Competition between these two processes is exponentially dependent on the temperature, due to a minor T dependence of the former and an Arrhenius-type dependence of the latter. At sufficiently high temperatures, the carrier transport via the conduction or valence band predominates.

If the mean free path of carriers is given by capture at impurities rather than by scattering, the conductivity can be described as a motion from one impurity center to another, but with electron transport *through the conduction band*[2] as illustrated in Fig. 1b (Fritzsche and Cuevas 1960; Butcher 1972). It can also be described as due to inelastic scattering at Coulomb-attractive centers, with phonon emission causing carrier capture. The corresponding carrier mobility is thermally activated:

$$\mu = \mu_0 \exp\left(-\frac{\Delta E_{\text{trap}}}{kT}\right), \tag{11}$$

where μ_0 is an effective mobility given by equivalent scattering mechanisms of carriers within the band, and ΔE_{trap} is the thermal activation energy of the trap.

Density Dependence of Hopping When the density of impurities increases, tunneling from center to center becomes more probable. The tunneling transport is accomplished by *hopping* from one to the adjacent center, resulting in a conductivity

$$\sigma_{\text{hop}} = \sigma_{0,\text{hop}} \exp\left(-\frac{\Delta E_{\text{hop}}}{kT}\right), \tag{12}$$

[2]In highly disordered semiconductors the motion may occur through excited states with greater overlap of their eigenfunctions.

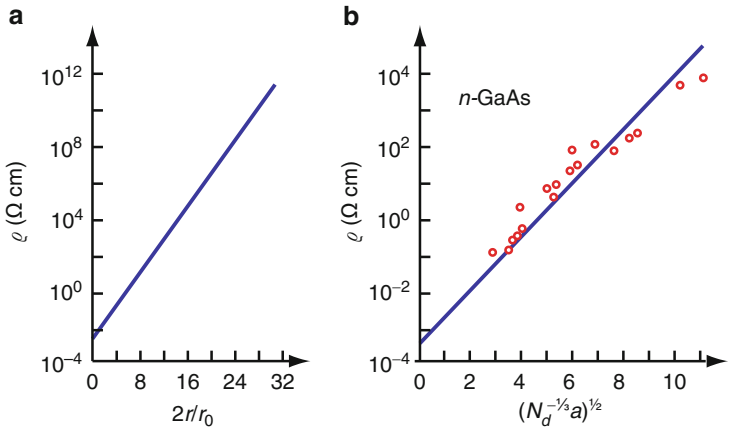

Fig. 3 (**a**) Calculated resistivity related to hopping conductivity as a function of the average separation between impurities. (**b**) Hopping resistivity as a function of the donor density in *n*-type GaAs (After Shklovskii and Efros 1984)

with ΔE_{hop} as the activation energy for hopping described below (Eq. 15) and with the preexponential factor given by

$$\sigma_{0,\text{hop}} = \sigma_{00} \exp\left(\frac{2r_c}{r_0}\right), \tag{13}$$

where r_0 is the fall-off radius of the impurity wavefunction ($= a_{\text{qH}}$ for quasi-hydrogen impurities). It is ~90 Å for Ga in Ge and ~47 Å for Cu in Ge; Cu has a larger ionization energy of ~40 meV. Also, r_c is the critical radius to establish a percolation path (see Sect. 4.2) from one electrode to the other, and can be estimated (McInnes and Butcher 1979) as

$$r_c \cong (0.865 \pm 0.015) N^{-1/3}, \tag{14}$$

where N is the density of the specific impurities between which hopping occurs.

The computed relation of the resistivity $\rho = \sigma^{-1}$ versus the mean separation of the impurities is shown in Fig. 3a. The corresponding relation of the measured resistivity for different donor densities N_d in GaAs is given in Fig. 3b (Shklovskii and Efros 1984); the solid curves gives the theoretical estimate according to Eqs. 13 and 14.

Activation Energy for Hopping When impurities are spaced close enough to permit tunneling, the levels split to form a narrow band. Therefore, tunneling to arbitrary neighbors usually requires a slight thermal activation energy (see Sect. 1.2.1). The activation energy can be interpreted as the energy from the Fermi level to the energy of the maximum of the density of empty-state distribution. Typically, it is on the order of a few meV and can be approximated for low compensation (Efros et al. 1972) by ~60% of the Coulomb energy at the average separation between the impurities:

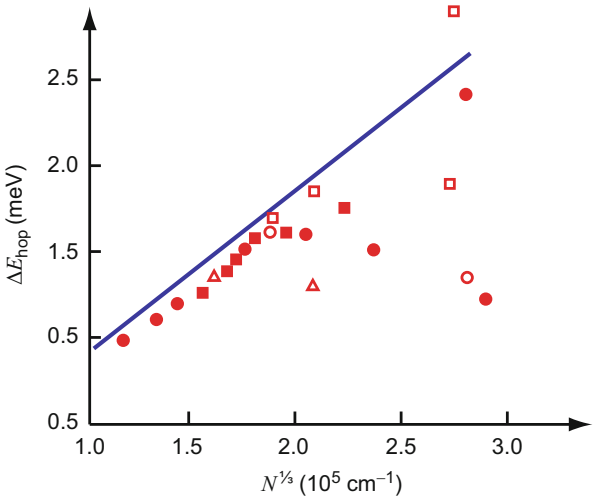

Fig. 4 Activation energy for hopping conduction in Ge doped with P, Ga, or Sb. The *solid line* is the theoretical dependence (Eq. 14) (After Shklovskii and Efros 1984)

$$\Delta E_{\text{hop}} \cong 0.61 \frac{e^2}{4\pi\,\varepsilon_{\text{stat}}\varepsilon_0}\left(\frac{4\pi}{3}N\right)^{1/3}. \tag{15}$$

The experimental values for ΔE_{hop} for Ge doped with P, Ga, or Sb are shown together with the theoretical curves (Eq. 15) in Fig. 4.

With a distribution of defects in space and energy, the relation becomes more complex and is relevant for amorphous semiconductors, see Sect. 4.3. For reviews, see Mott and Davis (1979), Shklovskii and Efros (1984) and Mott (1993).

A special type of hopping conduction relates to the hopping of small polarons and is discussed by Holstein (1959) and Schnakenberg (1968) (see also Sect. 5).

3 Heavily Doped Semiconductors

The basic concepts discussed in the previous sections apply also for highly doped semiconductors, however, in a modified fashion relating to the specific level distribution. This permits a number of more transparent theoretical approximations.

A semiconductor is heavily doped when the condition

$$N\ a_{\text{qH}}^3 \geq 1 \tag{16}$$

is fulfilled, which, dependent on the effective mass, is reached at vastly different doping densities in various semiconductors. For instance, $N\ a_{\text{qH}}^3 = 1$ requires $N = 5 \times 10^{15}$ cm^{-3} in n-type InSb and $N = 3 \times 10^{19}$ cm^{-3} in n-type Ge. In several semiconductors, the highly doped regime cannot be obtained by diffusion doping,

since clusters will form with limited solubility. Here, ion implantation or radiation damage can be used.

We will give a short review of the phenomena related to heavy doping in the following sections.

3.1 Intermediate Doping Range

The distinction between light and heavy doping can be made in relation to the disappearance of the gap in the impurity band and the transition from an activated semiconductivity to a quasi-metallic conduction (see Sect. 1.2.2). There is, however, a large intermediate range between the Mott-transition at $N\ a_{\mathrm{qH}}^3 \cong 0.02$ (► Eq. 64 of chapter "Equilibrium Statistics of Carriers") and the range of heavily doped semiconductors which starts at $N\ a_{\mathrm{qH}}^3 \cong 1$. In this intermediate range, some of the electrons are already delocalized.

The transition is related to the statistical distribution of the defects, which are frozen in and are located within the ensemble of free electrons, even at low temperatures. We will give some insight into this relation below. Other fluctuations are initiated at higher temperatures (*fluctuons*) and are reviewed by Krivoglaz (1974).

Density of States in Heavily Doped Semiconductors In highly doped semiconductors, there are two major contributions to the density of states: (1) the states which are due to the extended eigenfunctions of the defects and (2) the states which are due to the perturbation in the surrounding host lattice. The latter may be described by analyzing the influence of heavy doping on free electrons. This influence can be expressed by band-edge perturbation, through the modulation of the band edges by the Coulomb potential of the defects (Kane 1963; Halperin and Lax 1966). In highly doped semiconductors, clusters of charged impurities often dominate. The charges of such clusters, however, are *not* Coulomb point charges.

In turn, the potential fluctuation near charged impurities results in an inhomogeneous distribution of electrons. When the potential fluctuation is smooth within the deBroglie wavelength of free electrons, the electron gas can be described classically. Its density varies according to the density of states, which is increased at positions near an attractive center where the conduction band is lowered. Near attractive centers there will be more carriers, while near repulsive centers there will be less of the corresponding type. With high doping densities, the potential fluctuations will have a higher amplitude. Complete state filling of the valleys occurs at sufficiently low temperatures, whereas higher parts of the potential mountains extend above this "electron lake."

The density of states now becomes space-dependent

$$g(E,\mathbf{r})\ dE = \frac{(2m_n)^{3/2}}{2\pi^2\hbar^3}\sqrt{E + eV(\mathbf{r})}, \tag{17}$$

with the fluctuating potential determined by a screened Coulomb potential

$$V(\mathbf{r}) = \frac{e}{4\pi\,\varepsilon_{\text{stat}}\varepsilon_0\,\mathbf{r}} \exp\left(-\frac{r}{r_0}\right). \tag{18}$$

When averaging over the space-dependent potential, we obtain from Eq. 17 the density of states tailing into the bandgap (*Lifshitz tail*), as discussed in ▶ Sect. 3.1 of chapter "Optical Properties of Defects" and ▶ Sect. 1 of chapter "Defects in Amorphous and Organic Semiconductors".

3.2 Degenerate and Highly Compensated Heavily Doped Semiconductors

The highly doped semiconductor with shallow impurities is usually degenerate, i.e., the Fermi-level is shifted to well within the band. Depending on its position, the "lake" of electrons rises within a hilly terrain to fill only the lowest valleys as little lakes, or with a rising level connects more and more lakes until navigation from one electrode to the other becomes possible. This behavior is similar to that of a percolation conductivity, as described in Sect. 4.2.

When compensating a highly doped semiconductor, the level of the carrier lake within the modulated band drops, which causes a substantial decrease of the conductivity.

With sufficient compensation, the semiconductor reverts from metallic conduction to one with thermal activation over saddle points in the hilly terrain, as shown in Figs. 5 and 6. Here, carriers cannot contribute to percolation since they occupy only a small fraction of the volume, and tunneling is too expensive because of the high barriers between the remaining small puddles.

In completely compensated semiconductors, the potential fluctuation can increase further since the density of carriers is reduced below values, which are necessary for

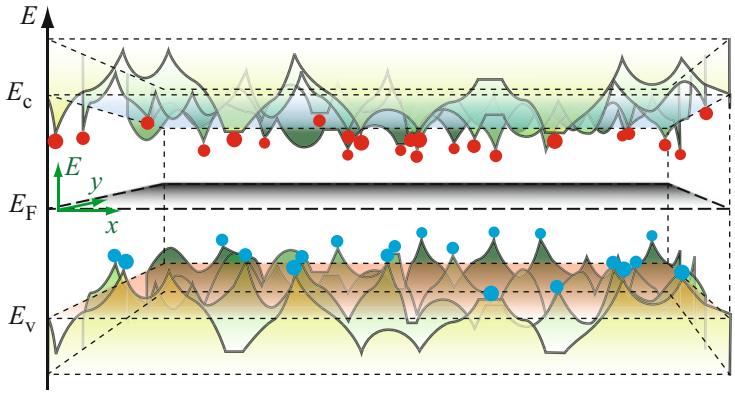

Fig. 5 Two-dimensional representation of the band-edge fluctuation in highly doped semiconductors. E_c and E_v refer to *average* values of conduction and valence band edges. *Red* and *blue circles* signify ionized donors and acceptors, respectively

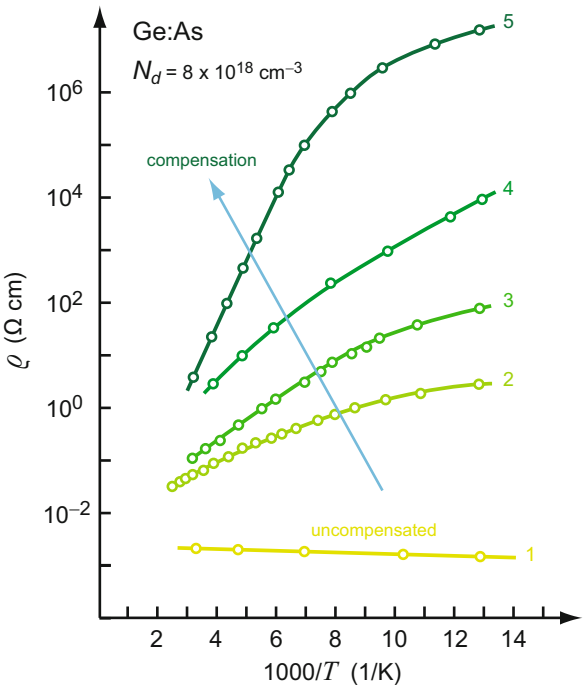

Fig. 6 Resistivity of an uncompensated (*lowest curve*) to more and more compensated samples of *n*-type Ge:As ($N_d = 8 \times 10^{18}$ cm^{-3}) as function of the inverse temperature (After Gadzhiev et al. 1972)

efficient screening. The maximum band fluctuation, however, is limited to $E_g/2$. Here, with penetration through the Fermi level, the deep valleys again become filled and screening reappears, thereby limiting any further increase in fluctuation of the band edges. For the effect of random defect density on the Fermi level in highly compensated semiconductors, see Donchev et al. (1997).

There is a large body of experimental and theoretical research on highly doped semiconductors, including the influence of light (*persistent photoconductivity* - Ryvkin and Shlimak 1973), of a magnetic field (*quantum screening* - Horring 1969, Aronzon and Chumakov 1994), and of low-temperature conductivity.

The carrier transport in such macroscopically fluctuating potentials is similar to that in semiconducting glasses (Ryvkin and Shlimak 1973, Overhof and Beyer 1981). In the following sections, we will analyze such transport in more detail.

4 Transport in Amorphous Semiconductors

The carrier transport in semiconducting glasses deserves a separate discussion because of the lack of long-range order and the high density of defects specific to the amorphous material. This does not permit simple translation of the effective-mass picture and requires a reevaluation of carrier transport and scattering concepts.

There are two aspects with direct influence on the carrier transport: (1) the strong tailing of states into the bandgap, and (2) the absence of specific doping-induced defects in amorphous chalcogenides.

The *tailing of states* from the band into the bandgap is rather smooth and does not show a well-defined band edge. This necessitates a more careful analysis of the mobility at different energies. At higher energies within the conduction band – i.e., closer to the surface of the Brillouin zone (see below for justification) – the electrons are quasi-free, except for scattering events, and have a mean free path λ larger than the interatomic spacing. Here, $\lambda\, k \gg 1$, and k may be used, albeit with some caution (Mott and Davis 1979).

With decreasing electron energy, the scattering probability increases, with scattering on potential fluctuations due to noncrystalline structures. Hence, the mean free path becomes comparable to the interatomic distance, and $\lambda\, k \cong 1$. Here, k is no longer a good quantum number.[3] Substantial differences between the crystalline and the amorphous semiconductor become important. Therefore, the carrier transport must now be described in terms of a transport between *localized states*; the Mott-Anderson localization threshold is reached (see ► Sect. 1.2 of chapter "Defects in Amorphous and Organic Semiconductors").

In taking a slightly different point of view, we expect the band states near the *edge* to become *perturbed* with a concurrent widening or narrowing of the bandgap, depending on the local degree of disorder. With charging of these defects, the Coulomb potential creates band undulations, as shown schematically in Fig. 5 (Böer 1972). In amorphous semiconductors with a much lower density of charged centers, a similar mountainous profile of the near-edge band states results from the local stress and other defect-induced perturbations.

When the Fermi- or quasi-Fermi level is moved above the lowest valleys of this edge (discussed in more detail in Sect. 4.2), these valleys will fill up with carriers. Assuming that only near the surface of such "lakes" a carrier transport is possible, one recognizes that a continuous current can only flow when the Fermi-level rises enough to permit a *percolation path* from one to the other electrode (Fig. 7a–c); much below the "edge" carriers are trapped. We will now refine this roughly stated model.

4.1 The Mobility Edge

Carriers are able to travel readily when the eigenfunctions of traps overlap. There are two arguments for a larger overlap of shallower traps: (1) they usually have a larger

[3] In a crystalline structure, k, when closer to the center of the Brilloin zone, represents points in real space farther away from the unit cell; in this case long-range deviation from periodicity becomes important. In contrast, when $\lambda\, k \cong 1$, the wavenumber is closer to the boundaries of the Brillouin zone; wheras in real space, the corresponding points are closer to the unit cell and the structure of the amorphous material resembles more that of a crystal.

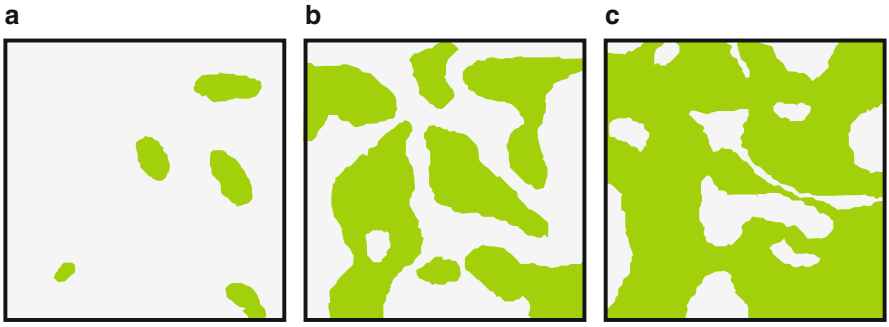

Fig. 7 Percolation regions (*green*), which become larger and interconnect with increasing energy from (**a**) to (**c**), connect as puddles in a hilly terrain to form small and larger lakes when the water level rises, finally leaving only small islands near the highest points of the terrain

fall-off radius of their eigenfunctions and (2) they are more plentiful, diminishing the intertrap distance. With an exponentially decreasing trap distribution, and with an adequately large overlap of shallow traps, the carrier transport through such shallow centers is almost band-like.

At slightly deeper trap levels, the carrier transport proceeds from trap to neighboring trap and has a diffusive character, with a diffusion constant given by the exchange frequency ν_{trap}:

$$D = \frac{\nu_{\text{trap}}\, a_{\text{trap}}^2}{6}; \tag{19}$$

here a_{trap} is the distance between these traps.

Carriers in yet deeper traps will have to penetrate through increasingly thicker barriers via tunneling. Finally, such carrier transfer via tunneling becomes negligible and requires thermal excitation into higher states.

In summary, the type of carrier transport depends on the depth of the traps between which such transport takes place. Carriers are significantly more mobile in shallower traps. There is a major step in the mobility of carriers between "localized" deeper and "extended" shallow trap states. This step at an energy E_μ is referred to as the *mobility edge*; see also ▶ Sect. 1.3 of chapter "Defects in Amorphous and Organic Semiconductors".

A material in which the Fermi level at $T = 0$ K coincides with the mobility edge is called a *Fermi glass*. This material displays metallic conductivity.

The distance between two defect centers at the mobility edge is approximately that of the nearest neighbors (Mott and Davis 1979), yielding for approximately cubic atom configurations (see ▶ Sect. 3.1 and ▶ Eq. 80 of chapter "Crystal Defects"):

$$D_\mu \cong \frac{\nu_\mu\, a^2}{6}, \tag{20}$$

with the tunneling frequency ν_μ approximated by the atomic electron frequency

$$\nu_\mu \cong \frac{\hbar}{m_0 a^2}. \tag{21}$$

We are *not* assuming hydrogen-like defects here. Therefore, tunneling is much reduced, and the distance of defects centers between which tunneling becomes significant can no longer be much larger than the normal interatomic distance *a.* Using the Einstein relation, this yields, as an order of magnitude estimate for the mobility at the mobility edge,

$$\mu_{\text{edge}} = \frac{e\ D_\mu}{kT} \cong \frac{e\ \hbar}{6 m_0 k T} \cong 7.5 \times \left(\frac{300\,\text{K}}{T}\right)\ \left(\text{cm}^2\,\text{V}^{-1}\,\text{s}^{-1}\right), \tag{22}$$

Electrons that are excited much above the mobility edge contribute to the current, as they do in a crystal, by being scattered at defects, and usually have a mean free path that is much larger than the interatomic distance. Electrons closer to the mobility edge contribute via exchange interaction to neighboring traps, and electrons that have relaxed much below the mobility edge contribute through tunneling or after thermal activation.

Since the mobility decreases very steeply at the mobility edge, whereas the density of states does not, it is customary to identify the *bandgap* in amorphous semiconductors as a *mobility gap*, i.e., the distance between the mobility edges for electrons and holes.

4.2 Diffusive Carrier Transport and Percolation

We will now look a bit closer at the carrier transport around the mobility edge E_μ. With decreasing trap energy E_{trap}, the trap density is reduced and the average distance between these defects is increased. At any given energy, the distance will fluctuate about an average value, making carrier transfer preferred in directions in which the distance is shortest. With further decreasing E_{trap}, preferred paths become rarer. The carrier has to move in a diffusive path along preferred intertrap connections. This indicates that the carrier motion, which was randomly diffusive at higher energies, now becomes direction-selective toward the closest neighbor, thereby reducing the effective diffusion constant. Finally, the path connecting the two electrodes will be broken. From this point on, thermally activated conductivity becomes the sole possibility for carrier transport.

The selection of paths between neighboring sites at the mobility edge is significant in that it is a determinant of the *Hall mobility.* In amorphous semiconductors, the Hall effect cannot be calculated from Lorentz forces, but must be computed from quantum-mechanical jump probabilities between localized states (Grünewald et al. 1981). Paths following the Lorentz force become *slightly* preferred. Because of this structure-determined path selection, the Hall voltage becomes dependent on the average microscopic geometry of the atomic arrangement. An anomalous sign of

the Hall effect may occur at weak fields for the mean free path below a critical magnitude (Okamoto et al. 1993). Mott (1991) has shown that the sign anomaly of the Hall coefficient in α-Si:H should be expected when the disorder causing the mobility edge originates from stretched bonds. With a scattering length of 20 Å in such amorphous materials at the mobility edge, only 1% of the bonds need to be stretched to produce such anomaly in the sign. Also preferred even- or odd-numbered rings (see ▶ Sect. 3.1 of chapter "The Structure of Semiconductors") cause a sign reversal of the Hall effect for *n*- or *p*-type material (see Dresner 1983).

Percolation We return to the carrier transport near the mobility edge. When filling traps by raising the Fermi-level, carrier diffusion is eased. This would appear homogeneously throughout the semiconductor if it were not for the mountainous profile of the potential, as illustrated in Fig. 5. Here, in a mountain, the mobility edge is pushed above the Fermi-level, whereas in a valley, the Fermi-level lies above the mobility edge. In these lakes, the mobile electrons show diffusive motion along the surface of the lakes, but have to tunnel through the mountains. This type of transport, which can be understood from classical arguments (Broadbent and Hammersley 1957), is commonly referred to as *percolation*. For a review, see Shante and Kirkpatrick (1971) or Böttger and Bryksin (1985).

The analysis of percolation was facilitated by the simple model of Miller and Abrahams (1960), using a network of random resistors and Kirchhoff's law to calculate the corresponding resistivity between the electrodes in a semiconductor with percolating conductivity. Many aspects of carrier percolation can be discussed in the frame work of *fractal networks*, i.e., a network of resistors in which a statistically increasing number of the interconnecting resistors are omitted. Multi-fractality in carrier transport at the mobility edge in amorphous semiconductors is discussed by Huckestein and Schweitzer (1993).

4.3 Activated Mobility

Further below the mobility edge, the defect centers are sufficiently separated so that tunneling between them can be neglected compared to the thermal excitation into levels near the mobility edge. From here, electrons can be retrapped, excited again, etc. This process can be described as *thermally activated hopping*[4] and requires a periodic interplay with phonons, i.e., carriers alternately absorb or emit phonons. Consequently, the hopping mobility depends exponentially on the temperature. For excitation from centers at an energy E_{trap}, we obtain

[4]Hopping conduction can also involve small polarons which move by hopping from site to site, ions which hop from interstitial to interstitial site, electrons which hop between soliton-bound states in one-dimensional conductors (acetylene) (Kivelson 1982), or Frenkel excitons in molecularcrystals (see Sect. 5 and references in Böttger and Bryksin 1985).

$$\mu_{\text{hop}} = \mu_0 \exp\left(-\frac{E_\mu - E_{\text{trap}}}{kT}\right). \tag{23}$$

The thermally activated hopping mobility can be described in the form of a diffusion relation (Butcher 1972):

$$\mu_{\text{hop}} = \frac{e}{kT} D_{\text{hop}} = \frac{e}{kT} \frac{\nu_{\text{hop}} r_{\text{hop}}^2}{6}. \tag{24}$$

The thermally activated effective hopping frequency is given by

$$\nu_{\text{hop}} = \frac{\omega_{\text{phon}}}{2\pi} \exp\left(-2\frac{r_{\text{hop}}}{r_0} - \frac{W_{\text{hop}}}{kT}\right), \tag{25}$$

where W_{hop} is the average energy difference between the two states for hopping, r_{hop} is the hopping distance, r_0 is the radius of the center, and ω_{phon} is an effective phonon frequency to match the energies of initial and scattered states. For hops of distance r_{hop}, the corresponding hopping energy is given by the band width of centers located at the Fermi energy $\Delta E_{\text{B}}(E_{\text{F}})$, which in turn is given by

$$W_{\text{hop}} = \Delta E_{\text{B}}(E_{\text{F}}) = \frac{3}{4\pi\, r_{\text{hop}}^3 g_N(E_{\text{F}})}, \tag{26}$$

with $g_N(E_{\text{F}})$ (dimension $\text{eV}^{-1}\,\text{cm}^{-3}$) the density of states for defects with an energy at the Fermi level, from which such activation makes the largest contribution to the mobility (see Mott 1969, Pollak 1972).

Variable Range Hopping In amorphous semiconductors with the Fermi level below the mobility edge, thermal activation becomes essential to carrier transport. With reduced temperature, the width of the energy band decreases, thereby involving less centers, i.e., the distance between the active centers increases (Mott 1968, 1969). The average hopping distance, which maximizes the hopping rate, is given by

$$\overline{r}_{\text{hop}} = \left(\frac{3\ r_0}{2\pi\ g_N(E_{\text{F}})\ kT}\right)^{1/4}. \tag{27}$$

This results in a hopping frequency of

$$\nu_{\text{hop}} \propto \exp\left(-\frac{C}{(kT)^{1/4}}\right), \text{with} C = 2\left(\frac{3}{2\pi}\right)^{1/4} \left(\frac{1}{r_0^3 g_N(E_{\text{F}})}\right)^{1/4}. \tag{28}$$

Introducing this relation into Eq. 23, we obtain a hopping mobility

$$\mu_{\text{hop}} = \mu_0 \exp\left(-\frac{T_0}{T}\right), \tag{29}$$

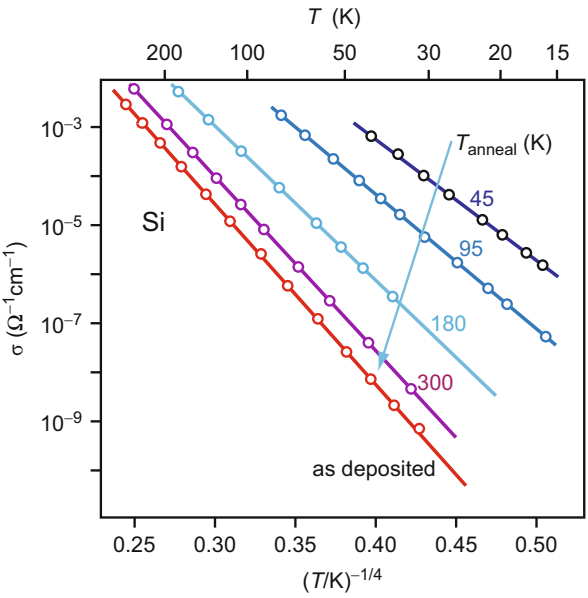

Fig. 8 Electrical conductivity of amorphous Si as a function of $T^{-1/4}$. Family parameter is the annealing temperature after damage with Si^+ bombardment (*uppermost curves*) (After Apsley et al. 1978)

which is experimentally observed in some of the amorphous semiconductors (see Fig. 8). In thin layers, the $T^{-1/4}$ relation changes to a $T^{-1/3}$ relation (Knotek et al. 1973). Here, percolation paths are cut open by the layer surfaces normal to the current flow (Hauser 1975). For a review of hopping conduction, see Böttger and Bryksin (1985); for variable-range hopping in *n*-channel α-SiGe quantum well structures, see Shin et al. (1999).

Hopping Mobility of Polarons The strong interaction of trapped carriers with phonons suggests the involvement of polarons in the carrier transport of amorphous semiconductors (Emin 1975, Mott and Davis 1979). In certain amorphous semiconductors, the carrier transport may also be caused by hopping of bipolarons (Schlenker and Marezio 1980, Elliott 1977, and Elliott 1978).

Dispersive Carrier Transport One of the most convincing arguments about the carrier transport involving a quasi-exponential trap distribution stems from experiments with excess carriers, e.g., injected or photo-excited carriers. These are trapped, reemitted from shallow traps, retrapped, and so on; during the period between trapping, they are mobile and drift in an electrical field. The first carriers that traverse the device have not been trapped, followed by carriers that have been trapped once, twice, etc. Consecutive trapping causes further slow-down of carrier traversal. When being retrapped, energy is dissipated by emitting phonons, and successively deeper traps are filled; from here escape is much slower. This behavior results in a typical distribution of these excess carriers as a function of the time while in transit, in agreement with the experiment. This confirms the intimate involvement of a trap distribution in carrier transport.

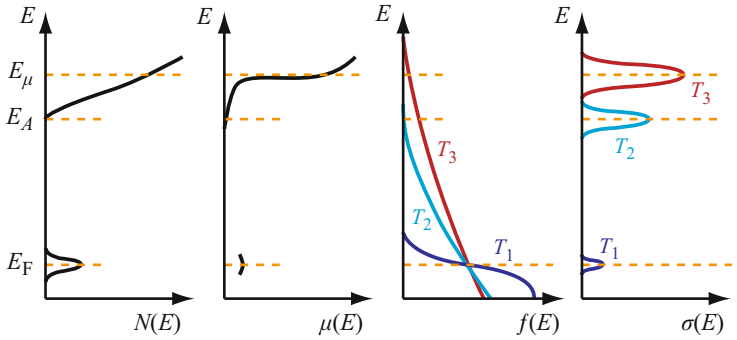

Fig. 9 Typical carrier distributions resulting in three different modes of conductivity at temperatures T_1, T_2, and T_3

Transport with a nonconstant hopping rate due to multiple trapping of carriers into progressively deeper states is referred to as *dispersive transport*. The change in hopping rates effects the broadening of a generated carrier ensemble. We will return to this subject when we discuss carrier kinetics in ▶ Sect. 1.1.3 of chapter "Dynamic Processes". For a review, see Tiedje (1984).

4.4 Temperature Dependence of the Conductivity

The relative magnitude of the different contributions to the conductivity is a function of the temperature. This is depicted in Fig. 9, in which the Fermi level remains pinned.

(a) At low temperatures (T_1), only carriers near E_F can contribute to the conductivity. Since pinning of the Fermi level requires a high density of defect states at E_F, such conductivity is similar to the impurity conduction in crystalline semiconductors. We can distinguish two cases of this *impurity conductivity*:

(a1) The impurity density near E_F is large enough to permit sufficient tunneling within a band of width ΔE_1; then impurity conduction similar to a crystalline semiconductor dominates, with

$$\sigma = \sigma_{a1} \exp\left(-\frac{\Delta E_1}{2\ kT}\right). \tag{30}$$

(a2) The impurity density is smaller and its bandwidth is larger than kT; then *variable-range hopping* occurs with the characteristic $(kT)^{-1/4}$ dependence:

$$\sigma = \sigma_{a2} \exp\left(-\frac{C}{\sqrt[4]{kT}}\right), \tag{31}$$

with C as given by Eq. 28. Such a dependence is shown in Fig. 8.

(b) At medium temperatures (T_2), sufficient carriers are excited into tailing states near E_A. They show sufficient overlap for tunneling, so that hopping is activated. With ΔE_2 as the activation energy for hopping, we obtain

$$\sigma = \sigma_{\mathrm{b}} \exp\left(-\frac{E_A - E_{\mathrm{F}} - \Delta E_2}{kT}\right). \tag{32}$$

However, since $E_A - E_{\mathrm{F}}$ is usually much larger than ΔE_2, one observes a constant slope in the $\ln(\sigma)$ versus $1/T$ diagram.

(c) At higher temperatures (T_3), when sufficient carriers are excited into non-localized, i.e., band states with an energy above the mobility-edge energy E_μ, the conductivity is given by

$$\sigma = \sigma_{\mathrm{c}} \exp\left(-\frac{E_\mu - E_{\mathrm{F}}}{kT}\right). \tag{33}$$

(d) With further increasing temperatures, the mobility may increase sufficiently above the saddle point between the undulating band edges to provide yet one more significant contribution to the conductivity:

$$\sigma = \sigma_{\mathrm{d}} \exp\left(-\frac{E'_{\mathrm{g}}}{2kT}\right), \tag{34}$$

where E'_{g} is a shifted effective bandgap energy: the mobility gap related to the mobility edges of electrons and holes. The pre-exponential factors are

$$\sigma_{\mathrm{a2}} = e^2 \omega \; N(E_{\mathrm{F}}) \; \overline{r}^2, \tag{35}$$

for variable range hopping (see Eq. 27),

$$\sigma_{\mathrm{b}} = 0.03 \frac{e^2}{\hbar \lambda_i}, \tag{36}$$

for hopping from tailing states, and

$$\left.\begin{matrix}\sigma_{\mathrm{a1}} \\ \sigma_{\mathrm{c}}\end{matrix}\right\} = \sigma_{\min} \cong \frac{e^2}{2\pi^2 \hbar a_{\mathrm{qH}}} \cong \frac{610}{a_{\mathrm{qH}}/\text{Å}} \quad \left(\Omega^{-1}\,\mathrm{cm}^{-1}\right) \tag{37}$$

for band conductivity. Finally,

$$\sigma_{\mathrm{d}} = \frac{e^2 \; g_N\left(E'_{\mathrm{g}}\right) \; kT \; \tau_e}{m_n} \tag{38}$$

for conduction above the saddle points of the band edges. Here, $\sigma_{\min}$ is the *minimum metallic conductivity* (see Mott and Davis 1979), τ_e is the energy-relaxation time, and $g_N\left(E'_g\right)$ is the joint density of states at E'_g, the shifted effective bandgap energy.

The type of predominant conductivity depends on material preparation (Connell and Street 1980). This becomes rather sensitive in tetrahedrally bound amorphous semiconductors, such as α-Ge:H or α-Si:H, where a wide range of $\sigma(T)$ behavior is observed, depending on deposition parameters, doping, hydrogenation, and annealing treatments (LeComber et al. 1972; Bullot and Schmidt 1987).

5 Charge Transport in Organic Semiconductors

Organic semiconductors comprise small-molecule crystals and polymers. Quite a few of them have been obtained as single crystals and highly purified to obtain their intrinsic semiconductor properties (▶ Sect. 1.5 of chapter "The Structure of Semiconductors"). Most organic solids are excellent insulators and become semiconductive only after doping (Pope and Swenberg 1982). Also organic polymers show semiconducting properties (Goodings 1976). They typically consist of polymer chains with a semiconducting backbone. Organic semiconductors are employed today in a wide field of applications, e.g., in organic LEDs (OLEDs) and displays, radio-frequency tags, solar cells, and integrated devices (Sirringhaus et al. 1998); for reviews see Hung and Chen (2002), Gather et al. (2011), Arias et al. (2010), Peumans et al. (2003), and Hains et al. (2010).

Conductance in organic semiconductors is governed by disorder. Even in perfect small-molecule crystals, the weak intermolecular van der Waals bonds give rise to a dynamical disorder which affects the mobility of carriers. Highly pure single crystals hence show generally an increase of mobility at decreased temperature. In contrast, less ordered organic solids exhibit an *decrease* of the mobility at lower temperatures due to localization of carriers and a required thermal activation for transport. We consequently observe both band conductance and hopping conductance in organic semiconductors.

Carriers in organic semiconductors couple strongly to molecular oscillations, suggesting a polaron-state contribution (Spear 1974). An early review of the theory of carrier mobility in organic semiconductors is given by Druger (1975). Karl (1984) gives a critical review of mobility and other physical data for both one-component and mixed organic semiconductors. A recent comprehensive review is given by Bässler and Köhler (2012).

5.1 Band Conductance in Organic Crystals

Band conductance is found particularly in small-molecule crystals. These are predominantly van der Waals bonded (▶ Sect. 3.3 of chapter "Crystal Bonding"); some of them have other bonding superimposed, such as ionic, hydrogen, and charge-

transfer bonding. We distinguish single-component and two-component (charge-transfer) semiconductors. The first group contains the classical organic semiconductors, such as the acenes (▶ Sect. 1.5 of chapter "The Structure of Semiconductors"), which show comparatively high mobilities; the second group includes highly conductive compounds, some of which show semiconductor-metal transitions and even superconductivity (▶ Sects. 1.1 and ▶ 2 of chapter "Superconductivity").

5.1.1 Single-Component and Two-Component Semiconductors

Single-Component Semiconductors. Single-component organic crystals are usually good insulators, but may become photoconductive with sufficient optical excitation. The class of aromatic hydrocarbons like the acenes has been more thoroughly investigated. They have bandgap energies between 2 and 5 eV (see ▶ Sect. 3 of chapter "The Origin of Band Structure") and are considered a class of one-dimensional conductors (Kivelson and Chapman 1983), albeit with a comparably small anisotropy ratio. The bandgap energy of organic semiconductors can rarely be determined by optical absorption, since valence-to-conduction band transitions are masked by transitions to excited molecular states referred to as excitons (Davidov 1962), which lie within the bandgap and do not support charge transport. Transport bandgap and optical bandgap are hence distinguished, see ▶ Sect. 4.1 of chapter "Bands and Bandgaps in Solids." The transport bandgap can be measured directly from the threshold of intrinsic photoconductivity (Marchetti and Kearns 1970) or from photoelectron spectroscopy.

The mobility is usually low compared to inorganic semiconductors, for electrons and holes typically in the 10^{-2} to 10 $cm^2/(Vs)$ range at 300 K, and falls with increasing temperature.

Two-Component Semiconductors Two-component semiconductors consist of pairs of complementary molecules with large differences in their redox properties: the organic molecules with a low ionization energy acts as electron donors D and the other molecules with a high electron affinity act as acceptors A. Such a combination produces organic crystals that can show very low or vanishing activation energies and comparatively high conductivities. The crystals are formed by a sandwich-like stacking of planar molecules, where donors and acceptors form $D^{\delta+}A^{\delta-}D^{\delta+}A^{\delta-}$ structures, or they are located in separated stacks, i.e., the stacking contains $D^{\delta+}D^{\delta+}\ldots$ and $A^{\delta-}A^{\delta-}\ldots$ complexes for segregated stacking with face-to-face stacks. δ denotes the transferred charge per molecule in units of elementary charges. The charge transfer (CT) may be incomplete, yielding two limiting cases: weak CT complexes and strong CT complexes, also referred to as radical ion salts (Soos 1974).

In *radical ion salts*, an organic radical cation (such as perylene$^+$) is combined with a counter anion (such as a halogen or PF_6^-), or an organic radical anion (such as $TCNQ^-$) is combined with a counter cation. The solids have a pronounced ionic character, i.e., δ is often close to 1; usually $\delta < 1$ for conductive radical ion salts.

Charge-transfer complexes with δ significantly smaller than unity can show high conductivities, caused by the incomplete charge transfer between D and A, which

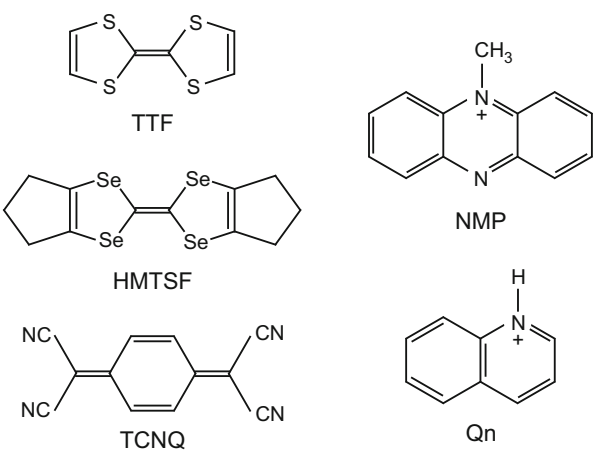

Fig. 10 Structure of some typical organic donor and acceptor molecules in charge-transfer crystals: Tetrathiofulvalene (*TTF*), Hexamethylenetetra-selenofulvalene (*HMTSF*), Tetracyanoquinodimethan (*TCNQ*), *N*-methylphenazinium (*NMP*), Quinolinium (*Qn*)

results for the ground state in partially filled bands. Typical donor and acceptor molecules that form such charge-transfer crystals are given in Fig. 10. Many such semiconductors have low-lying electronically excited states in which an electron is transferred from D to A. The charge-transfer transition in the excited state[5] may be written as

$$D\ A \rightarrow D^{+}A^{-} \text{ with } E_{\mathrm{CT}} = I_D - A_A - C, \tag{39}$$

where I_D is the ionization energy of the donor and A_A is the electron affinity of the acceptor (both in the gas phase), and C is a Coulomb binding-energy of the excited state. E_{CT} is the "energy gap" between the ground state and the excited charge-transfer state (Mulliken 1952).

The resulting structures are termed *neutral charge-transfer crystals*, typically with stacks of alternating D and A molecules: $DADADA\ldots$. The lowest excited state is $DADAD^{+}A^{-}DADA\ldots$; the respective activation energy for semiconductivity is typically (Kuroda et al. 1962)

$$E_s \cong \frac{1}{2} E_{\mathrm{CT}}. \tag{40}$$

The incomplete electron exchange and consequently partially filled bands results in a rather large semiconductivity – or even metallic conductivity. The resistivity of these semiconductors lies between 10^2 and 10^6 Ω cm at room temperature with a transfer-energy gap in the 0.1–0.4 eV range (Braun 1980). The conductivity is usually highly anisotropic, with the electron transfer-integral in the stacking direction typically a factor of 10 larger than in the direction

[5]The excited state has essentially ionic charge character.

perpendicular to the stacks (Keller 1977). Trapping is of minor importance in these semiconductors with a high carrier density (Karl 1984). The charge-transfer crystals provide an opportunity for fine tuning of the semiconductive properties by replacing TTF-type donors and TCNQ-type acceptors with other similar molecules (Bloch et al. 1977), which could render such materials attractive for some technical applications.

5.1.2 Carrier Mobility in Pure Organic Crystals

Organic molecules show a strong structural relaxation on introducing a charge. The band structure calculated for a crystal composed of weakly bonded neutral molecules may hence not be preserved in the presence of carriers. As a rule of thumb, band conductance occurs despite lattice relaxation if the transfer integral between molecules is sufficiently large: a large transfer integral delocalizes the carrier wavefunction over several molecules. A more quantitative estimate follows from the width W of the energy band for carrier transport. If the mean scattering time τ is in the range or smaller than $\hbar/W$, no wavevector $\mathbf{k}$ can be assigned to the carrier. The description in terms of conduction in a band with dispersion $E(\mathbf{k})$ hence requires

$$\tau \gg \frac{\hbar}{W}. \tag{41}$$

The bands in organic crystals are rather narrow due to a small amount of wavefunction overlap of π electrons, see ▶ Sect. 4.1 of chapter "Bands and Bandgaps in Solids"." Typical bandwidths W are in the range of some hundred meV (see Table 1), yielding $\tau > 10^{-15}$ s. If scattering results from molecular relaxation, τ is given by the characteristic time of molecular vibration; the carrier must leave the molecule before a significant relaxation and consequential trapping can occur. Equation 41 then reads $W \gg \hbar/\tau$. This yields bandwidths of 100–200 meV, a condition reasonable well fulfilled for crystals of acenes and comparable aromatic compounds.

A clear indication for band conduction is provided by the temperature dependence of the mobility. In inorganic semiconductors scattering at acoustic phonons leads to a $T^{-3/2}$ dependence of the carrier mobility (▶ Eq. 15 of chapter "Carrier Scattering at Low Electric Fields"). A comparable decrease of mobility at higher

Table 1 Bandwidth W of acene crystals for holes in the valence band (HOMO) and electrons in the conduction band (LUMO) (After Cheng et al. 2003)

	Bandwidth W	
Crystal	Valence band	Conduction band
Naphthaline	409	372
Anthracene	509	508
Tetracene	626	503
Pentacene	738	728

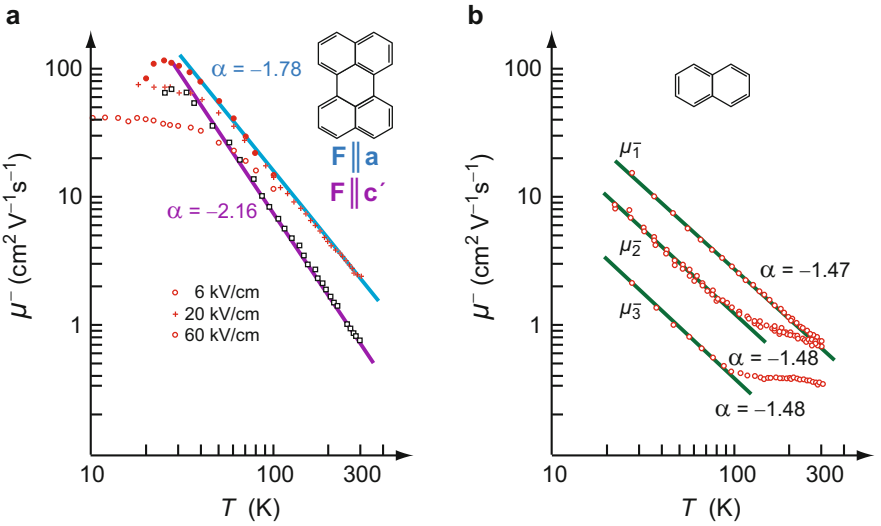

Fig. 11 Temperature dependence of the electron mobility (**a**) in a perylene crystal, and (**b**) in a naphthalene crystal (After Warta et al. (1985) and Karl (2001))

Table 2 Mobility μ in units of $cm^2\ V^{-1}\ s^{-1}$ for organic crystals at 300 K and exponent α of the temperature dependence according to Eq. 42

Crystal	Direction	Electrons		Holes	
		μ	α	μ	α
Naphthalene	*a*	0.62	−1.4	0.94	−2.8
	b	0.64	−0.55	1.84	−2.5
	c'	0.44	+0.04	0.32	−2.8
Anthracene	*a*	1.73	−1.45	1.13	−1.46
	b	1.05	−0.84	1.84	−1.26
	c'	0.39	+0.16	0.32	−1.43
Perylene	*a*	2.37	−1.78		
	b	5.53	−1.72		
	c'	0.78	−2.15		

temperature is observed for the carrier mobility in organic crystals with band conduction.

The mobility data in Fig. 11 show typical features of transport in organic crystals. The temperature dependence at low electric field F is described by a power law

$$\mu(T) = \mu_{300\mathrm{K}}\, T^{\alpha}, \tag{42}$$

where $\mu_{300\ \mathrm{K}}$ is the mobility at $T = 300$ K. The exponent α deviates somewhat from the ideal value of −3/2, see Table 2. The mobilities do not depend on the value of the electric field and show a pronounced anisotropy; the principal axes of the mobility tensor deviate slightly from the crystallograpic crystal axes. Typical mobilities are on

the order of $10^{-2}\ldots 10\ \mathrm{cm}^2/(\mathrm{Vs})$. Data for a large number of organic semiconductors are tabulated by Schein (1977); they decrease at higher temperature according to Eq. 42 with $0 > \alpha > -3$.

At high electric field F, the mobility shows a sublinear velocity-field relation, see Fig. 11a. The drift velocity of the carrier saturates at high fields, similar to the transport in inorganic semiconductors discussed in ▶ Sect. 1.1 of chapter "Carrier Scattering at High Electric Fields".

5.2 Hopping Conductance in Disordered Organic Semiconductors

Many organic compounds – small molecules or polymers – cannot be prepared as single crystals. They are usually prepared as thin films by evaporating or spin coating. The carrier mobility of these semiconductors is by orders of magnitudes lower than that of crystalline semiconductors considered above. In these semiconductors, the *static* disorder dominates at most temperatures, and the mobility *increases* for increasing temperature. The low coupling between the molecules in the solid state leads to a strong localization of the carriers on a molecule; transport occurs via a sequence of charge-transfer steps from one molecule to another, similar to the hopping between defect states in inorganic semiconductors. The transport properties are thus described by the formalism of hopping conductance developed for amorphous inorganic semiconductors (Sect. 4): the charge carriers are assumed to hop in a time-independent disordered energy landscape as illustrated in Fig. 5.

The basic difference between amorphous inorganic semiconductors and disordered organic semiconductors is the shape of the density of states (DOS). In an amorphous solid, the DOS is found to have a mobility edge and a tail of localized states with an *exponentially* decreasing distribution extending into the bandgap, see ▶ Figs. 2 and ▶ 3 of chapter "Defects in Amorphous and Organic Semiconductors" and Sect. 4. In contrast, the DOS in organic materials has a *Gaussian* shape:

$$g(E) = \frac{G_{\mathrm{tot}}}{\sqrt{2\pi}\sigma} \exp\left[\frac{(E - E_{\mathrm{center}})^2}{2\sigma^2}\right], \tag{43}$$

where G_{tot} is the total DOS, E_{center} is the center of the energy distribution, and σ is the variance of the distribution (Bässler 1993). Hopping of carriers is determined by both the energy difference ΔE and the spatial separation Δr of initial and final states; in addition, hopping is affected by an electric field F.

The hopping rate ν_{ij} between two localized states i and j depends on whether a hop-up ($\uparrow$) occurs with $\Delta E = E_j - E_i - eF(x_j - x_i)$ or a hop-down ($\downarrow$) with $\Delta E < 0$, where E_j and E_i are the energies within $g(E)$ at $F = 0$. Adopting the model of Miller and Abrahams (1960) we obtain

$$\nu_{ij}(\uparrow) = \nu_0 \exp\left(-2\gamma a \frac{\Delta r_{ij}}{a}\right) \exp\left(-\frac{E_j - E_i - eF(x_j - x_i)}{kT}\right), \tag{44}$$

$$\nu_{ij}(\downarrow) = \nu_0 \exp\left(-2\gamma a \frac{\Delta r_{ij}}{a}\right). \tag{45}$$

Here the constant γ is the spatial decrease of the wavefunction (invers Bohr radius for hydrogen-like wavefunctions), and a is the mean separation of localization sites. We note that a hop-down does not require a thermal activation.

Analogous to transport in amorphous inorganic semiconductors different transport regimes can be distinguished:

(a) Very low temperatures – *nearest neighbor hopping*: since $kT \ll \Delta E$, the spatial separation Δr controls the transfer, favoring next neighbors
(b) Low temperatures – *variable-range hopping*: the thermal energy kT allows for hopping within a narrow energy band around E_{center}, thereby relaxing the next-neighbor constraint
(c) Medium temperatures –*hopping in a wider energy range*: similar to (b) within a wider energy band, possibly opening percolation paths which are not restricted to next neighbors
(d) High temperatures – *multiple trapping and release*: carriers are excited from localized to extended states above the mobility edge, where band transport takes place until trapping at other localized states occurs. This regime requires a material where extended states exist.

The model of Bässler (1993) results in a thermally activated mobility

$$\mu = \mu_0 \exp\left[-\left(\frac{2\sigma}{3kT}\right)^2 + C\left(\left(\frac{\sigma}{kT}\right)^2 - \Sigma^2\right)\sqrt{F}\right] \tag{46}$$

determined by the spread σ of the energy distribution in the conducting band, the structural disorder parameter Σ, the applied electric field F, and the parameter μ_0 representing the mobility of the hypothetic not-disordered semiconductor at high temperature. The field dependence of Eq. 46 is comparable to the Poole-Frenkel effect (Frenkel 1938). For a more detailed review of various transport models, see Noriega and Salleo (2012). A review on experimental techniques for measuring transport properties is given by Coropceanu et al. (2007).

Polymers Typical examples of disordered organic semiconductors are the one-dimensional organic polymers, such as polyacetylene, as the simplest member (for *cis*-isomer see ▶ Fig. 15a of chapter "Crystal Bonding"), or the aromatic linear polymer poly(para-phenylenevinylene) (▶ Fig. 16 g of chapter "The Structure of Semiconductors"). Polyacetylene has been investigated most extensively – see the review by Heeger and MacDairmid (1980). It can easily be doped with donors or

acceptors, which are incorporated between the polymer chains of the *trans* isomer, resulting in controlled changes of the conductivity over 13 orders of magnitude up to $3 \times 10^3\ \Omega^{-1}\ \mathrm{cm}^{-1}$. At lower doping densities, devices with a *pn* junction can be formed from polyacetylene. At high doping densities, i.e., above 1%, a semiconductor-metal transition occurs. In the metallic state, polyacetylene has the optical appearance of a highly reflecting metal.

The typical structure of organic polymers has a bond alternation between conjugated single and double bonds within the backbone of the chain, see ▶ Sect. 3.3 of chapter "Crystal Bonding"; in polyacetylene there are two CH groups per unit cell, with one π electron for each CH group. At the boundary of two bond-alternation sequences with different phase, an unpaired electron is created; this bond alternation defect, illustrated in ▶ Fig. 14 of chapter "Defects in Amorphous and Organic Semiconductors," has attracted substantial interest as a manifestation of a *soliton*. Such a soliton can be described as a kink in the electron-lattice symmetry, rather than a spread-out transition; according minimum-energy calculations some spreading occurs, typically over about 10 lattice constants, remaining unchanged during the kink motion. Highly mobile, the soliton has a room-temperature hopping rate in excess of $10^{13}\ \mathrm{s}^{-1}$. The soliton seems to be responsible for a wide variety of unusual electrical, optical, and magnetic properties of these polymers. A short review is given by Heeger (1981).

Mobility in Polymers The mobility is widely measured using time-of-flight experiments. Such studies of disordered organic semiconductors show both dispersive and

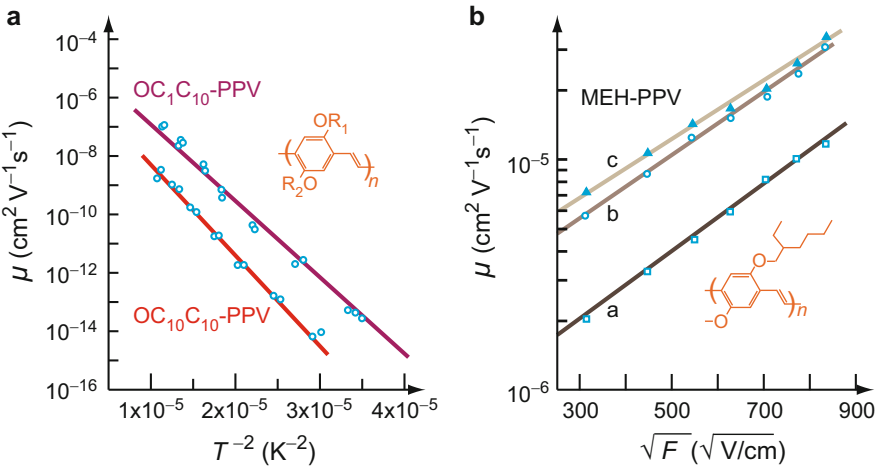

Fig. 12 Hole mobility in derivatives of PPV. (**a**) Mobility in derivatives with different side groups at zero electric field; OC_1C_{10}-PPV: $R_1 = CH_3$, $R_2 = C_{10}H_{21}$; $OC_{10}C_{10}$-PPV: $R_1 = R_2 = C_{10}H_{21}$ (After Blom and Vissenberg 2000). (**b**) Dependence of the hole mobility on the electric field *F* for MEH-PPV ($R_1 = C_8H_{16}$, $R_2 = CH_3$) prepared without (*a*) and with application of an electric field of 3 and 6 kV/cm for *b* and *c*; after Shi et al. (2006)

nondispersive components, depending on temperature, electric field, and chemical purity. Nondispersive carrier mobilities show typical features (Bässler 1993): a field-independent activated mobility at low fields, characterized by an activation energy, and a field-dependent contribution in the form of a stretched exponential at high fields F. These findings can in many cases be described by the empirical dependence

$$\mu \cong \mu_0 \exp\left[-\frac{E_A}{kT} + \beta\sqrt{F}\right], \tag{47}$$

with the zero-field mobility μ_0, an activation energy E_A, and the field-activation factor

$$\beta = B\left(\frac{1}{kT} - \frac{1}{kT_0}\right); \tag{48}$$

B and T_0 are empirical parameters. Since polymers are stable only in a very limited temperature range, the temperature dependence can often be described in this interval by different relations, such as Eqs. 46 or 47.

The hole mobility of the poly(paraphenylene vinylene) (PPV) is shown in Fig. 12. Holes dominate the current in many polymers. The polymer PPV is a prominent compound due to its electroluminescence properties; PPV derivatives are soluble and can be spin coated for, e.g., fabrication of organic LEDs. The mobility is reasonably described by a $\log(\mu) \propto T^{-2}$ dependence, although also an Arrhenius dependence $\log(\mu) \propto T^{-1}$ fits well (Blom et al. 1997); in the limited temperature range a clear distinction is not possible. The activation energies E_A for PPV derivatives (Eq. 47) range between 0.3 and 0.5 eV, and widths σ of the Gaussian DOS according to Eq. 46 are near 100 meV, with mean separations a of localization sites in the range 1.1 ... 1.7 nm (Blom and Vissenberg 2000). We note in Fig. 12 the comparatively low mobility of disordered organic semiconductors and the characteristic increase at higher temperature.

The enhancement of the mobility in an electric field is shown in Fig. 12b. The dependence on $F^{1/2}$ is well fulfilled. This behavior has also been observed from time-of-flight measurements in many molecularly doped polymers and amorphous glasses. An electrically induced polarization of MEH-PPV during the preparation of films significantly enhances the mobility.

6 Summary

Carrier transport is generally influenced by defects; however, in highly doped or disordered semiconductors, the carrier transport becomes *induced* by defects. If doping produces a well-defined predominant defect level with increasing density, it will split into two (bonding and antibonding) bands separated by an energy gap. Below a density to permit sufficient tunneling, excitation from the filled, lower impurity band into the conduction band is required for carrier transport. When the

impurity band is wider than $2kT$ and the Fermi level lies in the middle of this band, *variable range hopping* occurs: with decreasing T, the predominant excitation occurs from a narrower range of width kT of these centers, and causes a semilogarithmic slope $\propto T^{1/4}$. With increased defect density, a diffusive transport within the upper impurity band becomes possible; the conductivity in this band requires a small activation energy to bridge the gap. With further increase of the defect density, the carriers become delocalized, the gap disappears, and the conductivity within the impurity band becomes metallic.

In amorphous semiconductors, a similar tunneling-induced carrier transport can take place within the tail of states that extend from the conduction or valence band into the bandgap, when the states are close enough to each other to permit significant tunneling. Here carriers become delocalized. The edge at which delocalizing occurs is referred to as the mobility edge. At this edge, major carrier transport starts; below the mobility edge, carriers are trapped rather than being mobile.

With a statistical distribution of defects within semiconductors, at a given threshold, only some volume elements become conductive. With increasing temperature these volume elements will widen, will start to interconnect, and finally will provide an uninterrupted path from electrode to electrode. Such percolation character is typical for most of the conduction phenomena in highly doped or disordered semiconductors, which have a density-related threshold of conduction. The mobility of carriers in such semiconductors is typically on the order of 10 $cm^2/(Vs)$ or lower. At low temperatures it is determined by tunneling (hopping) from neighbor to neighbor and is very sensitive to the density of defects and their distribution in space and energy. At sufficiently high temperatures, carrier transport higher within the conduction or valence band may compete significantly with the conduction mechanisms described above. This band conduction may have a mean free path compatible to the one in crystalline semiconductors.

Organic semiconductors can be *single-component* materials, which can be doped, such as aromatic hydrocarbons (e.g., anthracene). These materials are good insulators and show photoconductivity. Another group of single-component semiconductors is comprised of certain linear polymers, such as polyacetylene. With doping this group can change its conductivity up to 13 orders of magnitude and can become metallic in electrical behavior and optical appearance. *Two-component* semiconductors contain molecules or molecular layers, which act as donors and others which act as acceptors. Variation of their donor/acceptor ratio can change the behavior from highly compensated to *n*- or *p*-type, with a wide range of conductivities, depending on the deviation from a donor to acceptor ratio of 1: 1. There is a great variety of such crystals that exhibit a broad range of properties, including metallic conductivity and, at low temperatures, superconductivity.

The carrier mobility in organic semiconductors is substantially lower than in good semiconducting inorganic compounds and typically is in the 10^{-3} to 10 $cm^2/(Vs)$ range. It is controlled by static and dynamic disorder. Small-molecule crystals show band conductance with a decreasing carrier mobility at increased temperature; it is affected by dynamic disorder and described by a power law similar to that of inorganic semiconductors. Films of small-molecules or polymer semiconductors

have dominating static disorder; they show hopping conductance with a typically very low mobility, which increases at higher temperatures.

References

Abrahams E, Anderson PW, Licciardello DC, Ramakrishnan TV (1979) Scaling theory of localization: absence of quantum diffusion in two dimensions. Phys Rev Lett 42:673

Adler D (1980) Electronic correlations, polarons, and hopping transport. In: Moss TS, Paul W (eds) Handbook on semiconductors, Theory and transport properties, vol 1. North Holland Publishing Company, Amsterdam, pp 805–841

Altshuler BL, Aronov AG, Lee PA (1980) Interaction effects in disordered Fermi systems in two dimensions. Phys Rev Lett 44:1288

Apsley N, Davis EA, Troup AP, Yoffee AD (1978) Electronic properties of ion-bombarded evaporated germanium and silicon. J Phys C 11:4983

Arias AC, MacKenzie JD, McCulloch I, Rivnay J, Salleo A (2010) Materials and applications for large area electronics: solution-based approaches. Chem Rev 110:3

Aronov AG, Mirlin DN, Nikitin LP, Reshina II, Sapega VF (1979) Determination of the inter-band transition time in the valence band of gallium arsenide. Sov Phys JETP 29:62

Aronzon BA, Chumakov NK (1994) Quantum effects and the phase diagram of the electronic system of highly compensated semiconductors in magnetic field. Physica B 194–196:1167

Bässler H (1993) Charge transport in disordered organic photoconductors. Phys Status Solidi B 175:15

Bässler H, Köhler A (2012) Charge transport in organic semiconductors. Top Curr Chem 312:1

Bloch AN, Carruthers TF, Poehler TO, Cowan DO (1977) The organic metallic state: some physical aspects and chemical trends. In: Keller HJ (ed) Chemistry and physics in one-dimensional metals. Plenum Press, New York, pp 47–85

Blom PWM, Vissenberg MCJM (2000) Charge transport in poly(p-phenylene vinylene) light-emitting diodes. Mater Sci Eng 27:53

Blom PWM, de Jong MJM, van Munster MG (1997) Electric-field and temperature dependence of the hole mobility in poly(p-phenylene vinylene). Phys Rev B 55:R656

Böer KW (1972) Perturbed bands in real semiconducting glasses. J Non-Cryst Sol 8–10:586

Böttger H, Bryksin VV (1979) Effective medium theory for the hopping conductivity in high electrical fields. Phys Status Solidi B 96:219

Böttger H, Bryksin VV (1980) Investigation of non-Ohmic hopping conduction by methods of percolation theory. Philos Mag B 42:297

Böttger H, Bryksin VV (1985) Hopping conduction in solids. VCH-Verlagsgesellschaft, Weinheim

Braun CL (1980) Organic semiconductors. In: Moss TS, Keller SP (eds) Handbook on semiconductors, Materials properties and preparation, vol 3. North Holland Publications, Amsterdam, pp 857–873

Broadbent SR, Hammersley JM (1957) Percolation processes I. Crystals and mazes. Proc Camb Philos Soc 53:629

Bullot J, Schmidt MP (1987) Physics of amorphous silicon-carbon alloys. Phys Status Solidi B 143:345

Butcher PN (1972) On the rate equation formulation of the hopping conductivity problem. J Phys C 5:1817

Cheng YC, Silbey RJ, da Silva Filho DA, Calbert JP, Cornil J, Brédas JL (2003) Three-dimensional band structure and bandlike mobility in oligoacene single crystals: a theoretical investigation. J Chem Phys 118:3764

Ching WY, Huber DL (1982) Numerical studies of energy levels and eigenfunction localization in dilute three-dimensional systems with exponential interactions. Phys Rev B 25:1096

Coropceanu V, Cornil J, da Silva Filho DA, Olivier Y, Silbey R, Bredas JL (2007) Charge transport in organic semiconductors. Chem Rev 107:926
Davidov AS (1962) Theory of molecular excitons. McGraw-Hill, New York
Donchev V, Shtinkov N, Germanova K (1997) Effect of random defect density fluctuations on the Fermi level in highly compensated semiconductors. Mater Sci Eng B 47:131
Dresner J (1983) Hall effect and hole transport in B-doped a-Si:H. J Non-Cryst Sol 58:353
Druger SD (1975) Theory of charge transport processes. In: Birks JB (ed) Organic molecular photophysics, vol 2. Wiley, London, pp 313–394
Efros AL, Shklovskii BI (1975) Coulomb gap and low temperature conductivity of disordered systems. J Phys C 8:L49
Efros AL, Shklovskii BI, Yanchev IY (1972) Impurity conductivity in low compensated semiconductors. Phys Status Solidi B 50:45
Elliott SR (1977) A theory of a.c. conduction in chalcogenide glasses. Philos Mag 36:1291
Elliott SR (1978) Defect states in amorphous silicon. Philos Mag B 38:325
Emin D (1975) Phonon-assisted transition rates I. Optical-phonon-assisted hopping in solids. Adv Phys 24:305
Frenkel J (1938) On pre-breakdown phenomena in insulators and electronic semi-conductors. Phys Rev 54:647
Fritzsche H, Cuevas M (1960) Impurity conduction in transmutation-doped *p*-type germanium. Phys Rev 119:1238
Gadzhiev AR, Ryvkin SM, Shlimak IS (1972) Fast-neutron-compensated *n*-germanium as a model of amorphous semiconductors. Sov Phys JETP Lett 5:428
Gather MC, Köhnen A, Meerholz K (2011) White organic light-emitting diodes. Adv Mater 23:233
Goodings EP (1976) Conductivity and superconductivity in polymers. Chem Soc Rev 5:95
Greenwood DA (1958) The Boltzmann equation in the theory of electrical conduction in metals. Proc Phys Soc Lond 71:585
Grünewald M, Thomas P, Würtz D (1981) The sign anomaly of the Hall effect in amorphous tetrahedrally bonded semiconductors: a chemical-bond orbital approach. J Phys C 14:4083
Hacker K, Obermair G (1970) Stark ladders in a one-band-model. Z Phys 234:1
Haegel NM, Samperi SA, White AM (2003) Electric field and responsivity modeling for far-infrared blocked impurity band detectors. J Appl Phys 93:1305
Hains AW, Liang Z, Woodhouse MA, Gregg BA (2010) Molecular semiconductors in organic photovoltaic cells. Chem Rev 110:6689
Halperin BI, Lax M (1966) Impurity-band tails in the high-density limit. I. Minimum counting methods. Phys Rev 148:722
Hauser JJ (1975) Hopping conductivity in amorphous carbon films. Solid State Commun 17:1577
Heeger AJ (1981) Semiconducting and metallic polymers: new science with potential for new technology. Comments Sol State Phys 10:53
Heeger AJ, MacDairmid AG (1980) Conducting organic polymers: doped polyacetylene. In: Alcàcer L (ed) The physics and chemistry of low-dimensional solids. Reidel, Dordrecht, pp 353–391
Holstein T (1959) Polaron band narrowing. Ann Phys 8:325. ibid 8:343
Horring NJ (1969) Quantum theory of static shielding of an impurity charge by an electron gas plasma in a magnetic field. Ann Phys 54:405
Hubbard J (1963) Electron correlations in narrow energy bands. Proc R Soc Lond A 276:238
Huckestein B, Schweitzer L (1993) Multifractality and anomalous diffusion at the mobility edge in disordered systems. J Non-Cryst Sol 164:461
Hung LS, Chen CH (2002) Recent progress of molecular organic electroluminescent materials and devices. Mater Sci Eng 39:143
Ioffe AF, Regel AR (1960) Non-crystalline, amorphous and liquid electronic semiconductors. Prog Semicond 4:237
Kane EO (1963) Thomas-Fermi approach to impure semiconductor band structure. Phys Rev 131:79
Karl N (1984) Organic semiconductors. Landoldt-Börnstein/Springer, Heidelberg

Karl N (2001) Charge-carrier mobility in organic crystals. In: Farchioni R, Grosso G (eds) Organic electronic materials: conjugated polymers and low molecular weight organic solids. Springer, Berlin, pp 283–326
Keller HJ (ed) (1977) Chemistry and physics in one-dimensional metals. Plenum Press, New York
Kivelson S (1982) Electron hopping in a soliton band: conduction in lightly doped $(CH)_x$. Phys Rev B 25:3798
Kivelson S, Chapman OL (1983) Polyacene and a new class of quasi-one-dimensional conductors. Phys Rev B 28:7236
Knotek ML, Pollak M, Donovan TM, Kurtzman H (1973) Thickness dependence of hopping transport in amorphous-Ge films. Phys Rev Lett 30:853
Knotek ML, Pollak M (1974) Correlation effects in hopping conduction: a treatment in terms of multielectron transitions. Phys Rev B 9:664
Krivoglaz MA (1974) Fluctuon states of electrons. Sov Phys Usp (Engl Transl) 16:856
Kubo R (1956) A general expression for the conductivity tensor. Can J Phys 34:1274
Kubo R (1957) Statistical-mechanical theory of irreversible processes. I. General theory and simple applications to magnetic and conduction problems. J Phys Soc Jpn 12:570
Kuroda H, Kobayashi M, Kinoshita M, Takemoto S (1962) Semiconductive properties of tetracyanoethylene complexes and their absorption spectra. J Chem Phys 36:457
LeComber PG, Madan A, Spear WE (1972) Electronic transport and state distribution in amorphous Si films. J Non-Cryst Sol 11:219
Lifshitz IM (1965) Energy spectrum structure and quantum states of disordered condensed systems. Sov Phys Usp (Engl Transl) 7:549
Maekawa S (1970) Nonlinear conduction of ZnS in strong electric fields. Phys Rev Lett 24:1175
Marchetti AP, Kearns DR (1970) Photoelectron emission from aromatic and metalloorganic hydrocarbons. Mol Cryst Liq Cryst 6:299
Mazuruk K, Benzaquen M, Walsh D (1989) Coulomb gap and screening in impurity bands. Solid State Commun 69:337
McInnes JA, Butcher PN (1979) Numerical calculations of dc hopping conductivity. Philos Mag B 39:1
Miller A, Abrahams E (1960) Impurity conduction at low concentrations. Phys Rev 120:745
Mott NF (1968) Conduction in glasses containing transition metal ions. J Non-Cryst Sol 1:1
Mott NF (1969) Conduction in non-crystalline materials. Philos Mag 19:835
Mott NF (1991) The sign of the Hall effect in amorphous silicon. Philos Mag B 63:3
Mott NF (1993) Conduction in non-crystalline materials, 2nd edn. Clarendon Press, Oxford
Mott NF, Davis EA (1979) Electronic processes in noncrystalline materials. Claredon Press, Oxford, UK
Mott NF, Kaveh M (1985) Metal-insulator transitions in non-crystalline systems. Adv Phys 34:329
Mulliken RS (1952) A comparative survey of approximate ground state wave functions of helium atom and hydrogen molecule. Proc Nat Akad Sci 38:160
Noriega R, Salleo A (2012) Charge transport theories in organic semiconductors. In: Klauk H (ed) Organic electronics II. Wiley-VCH, Weinheim, pp 67–104
Okamoto H, Hattori K, Hamakawa Y (1993) Hall effect near the mobility edge. J Non-Cryst Sol 164–166:445
Overhof H, Beyer W (1981) A model for the electronic transport in hydrogenated amorphous silicon. Philos Mag B 43:433
Peumans P, Yakimov A, Forrest SR (2003) Small molecular weight organic thin-film photodetectors and solar cells. J Appl Phys 93:3693
Pollak M (1972) A percolation treatment of dc hopping conduction. J Non-Cryst Solids 11:1
Pope M, Swenberg CE (1982) Electronic processes in organic crystals. Oxford University Press, Oxford
Priour DJ Jr (2012) Electronic states in one-, two-, and three-dimensional highly amorphous materials: a tight-binding treatment. Phys Rev B 85:014209

Pronin KA, Bandrauk AD, Ovchinnikov AA (1994) Electric-field-induced localization and non-perturbative response of a one-dimensional conductor. J Phys Condens Matter 6:4721
Rosenbaum TF, Andres K, Thomas GA, Bhatt RN (1980) Sharp metal-insulator transition in a random solid. Phys Rev Lett 45:1723
Ryvkin SM, Shlimak IS (1973) A doped highly compensated crystal semiconductor as a model of amorphous semiconductors. Phys Status Solidi A 16:515
Schein LB (1977) Temperature independent drift mobility along the molecular direction of As_2S_3. Phys Rev B 15:1024
Schlenker C, Marezio M (1980) The order–disorder transition of Ti^{3+}–Ti^{3+} pairs in Ti_4O_7 and $(Ti_{1-x}V_x)_4O_7$. Philos Mag B 42:453
Schnakenberg J (1968) Polaronic impurity hopping conduction. Phys Status Solidi B 28:623
Shante VKS, Kirkpatrick S (1971) An introduction to percolation theory. Adv Phys 20:325
Shi Q, Hou Y, Lu J, Jin H, Yunbai L, Yan L, Sun X, Liu J (2006) Enhancement of carrier mobility in MEH-PPV film prepared under presence of electric field. Chem Phys Lett 425:353
Shin D-H, Becker CE, Harris JJ, Fernández JM, Woods NJ, Thornton TJ, Maude DK, Portal J-C (1999) Variable-range hopping transport in modulation-doped n-channel $Si/Si_{1-x}Ge_x$ quantum well structures. Semicond Sci Technol 14:762
Shklovskii BI, Efros AL (1984) Electronic properties of doped semiconductors. Springer, Berlin
Sirringhaus H, Tessler N, Friend RH (1998) Integrated optoelectronic devices based on conjugated polymers. Science 280:1741
Soos ZG (1974) Theory of π-molecular charge-transfer crystals. Annu Rev Phys Chem 25:121
Spear WE (1974) Electronic transport and localization in low mobility solids and liquids. Adv Phys 23:523
Thouless DJ (1974) Electrons in disordered systems and the theory of localization. Phys Rep 13:93
Thouless DJ (1980) Resistance and localization in thin films and wires. J Non-Cryst Sol 35:3
Tiedje T (1984) Information about band-tail states from time-of-flight experiments. In: Willardson RK, Beer AC, Ji P (eds) Semiconductors and semimetals, vol 21C. Academic, New York, pp 207–238
Wang X, Wang B, Hou L, Xie W, Chen X, Pan M (2015) Design consideration of GaAs-based blocked-impurity-band detector with the absorbing layer formed by ion implantation. Opt Quant Electron 47:1347
Wannier GH (1960) Wave functions and effective hamiltonian for Bloch electrons in an electric field. Phys Rev 117:432
Warta W, Stehle R, Karl N (1985) Ultrapure, high mobility organic photoconductors. Appl Phys A Mater Sci Process 36:163